

# *Hydrogen sulfide inhibits the browning of fresh-cut apple by regulating the antioxidant, energy and lipid metabolism*

Article

Accepted Version

Creative Commons: Attribution-Noncommercial-No Derivative Works 4.0

Chen, C., Jiang, A., Liu, C., Wagstaff, C. ORCID:  
<https://orcid.org/0000-0001-9400-8641>, Zhao, Q., Zhang, Y.  
and Hu, W. (2021) Hydrogen sulfide inhibits the browning of  
fresh-cut apple by regulating the antioxidant, energy and lipid  
metabolism. *Postharvest Biology and Technology*, 175.  
111487. ISSN 0925-5214 doi:  
<https://doi.org/10.1016/j.postharvbio.2021.111487> Available at  
<https://centaur.reading.ac.uk/95960/>

It is advisable to refer to the publisher's version if you intend to cite from the work. See [Guidance on citing](#).

To link to this article DOI: <http://dx.doi.org/10.1016/j.postharvbio.2021.111487>

Publisher: Elsevier

All outputs in CentAUR are protected by Intellectual Property Rights law, including copyright law. Copyright and IPR is retained by the creators or other copyright holders. Terms and conditions for use of this material are defined in the [End User Agreement](#).

[www.reading.ac.uk/centaur](http://www.reading.ac.uk/centaur)

**CentAUR**

Central Archive at the University of Reading

Reading's research outputs online

1 **Hydrogen sulfide inhibits the browning of fresh-cut apple by**  
2 **regulating the antioxidant, energy and lipid metabolism**

3  
4 **Chen Chen<sup>a</sup>, Aili Jiang<sup>a</sup>, Chenghui Liu<sup>a</sup>, Carol Wagstaff<sup>b</sup>, Qiqi Zhao<sup>a</sup>,**  
5 **Yanhui Zhang<sup>a</sup>, Wenzhong Hu<sup>a\*</sup>**

6  
7 *<sup>a</sup>Key Laboratory of Biotechnology and Bioresources Utilization, Ministry of Education, College of*  
8 *Life Science, Dalian Minzu University, Dalian, 116600, China*

9 *<sup>b</sup>School of Chemistry Food & Pharmacy, Harry Nursten Building, University of Reading,*  
10 *Whiteknights, Reading, Berkshire, RG6 6DZ, UK*

11  
12  
13  
14  
15  
16 \*Corresponding author

17 Wenzhong Hu

18 Mailing address: College of Life Science, Dalian Minzu University, No. 18, Liaohe

19 West Road, Jinzhou New District, 116600, Dalian, P. R. China

20 Tel.: +86 411 87656213 E-mail: hwz@dlmu.edu.cn

21 **Abstract:** Surface browning is the primary limiting factor for the shelf-life of  
22 fresh-cut apple. Hydrogen sulfide (H<sub>2</sub>S) treatment is known to effectively inhibit the  
23 browning, however, little is known about the underlying molecular mechanism. In the  
24 present paper RNA-Seq technology was used to analyse the transcript expression  
25 profiles of control and H<sub>2</sub>S treated fresh-cut apple immediately after treatment (C0  
26 and S0) and 6 d of storage (C6 and S6) at 4 °C. The results identified 3782 and 1164  
27 differentially expressed unigenes (DEGs) in S0 vs. C0 and S6 vs. C6, respectively.  
28 Expression of most DEGs related to antioxidant systems and energy metabolism was  
29 up-regulated after H<sub>2</sub>S treatment, whilst expression of genes encoding polyphenol  
30 oxidase, peroxidase, lipid-degrading enzymes, such as lipoxygenase and  
31 phospholipase D, was repressed. Further quantitative real-time PCR testing validated  
32 the reliability of our RNA-Seq results. We therefore propose that H<sub>2</sub>S treatment  
33 inhibited the surface browning of fresh-cut apple by regulating antioxidant, energy  
34 and lipid metabolism to maintain the membrane integrity of the plant tissue.

35

36 **Keywords:** Fresh-cut apple; hydrogen sulfide, browning, transcriptome

37

## 38 **1. Introduction**

39

40 Fresh-cut apple, which contain phenolic components that have an antioxidant  
41 capacity in the fruit, have recently emerged as popular snacks in food service  
42 establishments, school lunch programs, and for family consumption (Guan and Fan,  
43 2010). However, they are more perishable than intact produce because apple fruit  
44 undergo enzymatic browning during minimal processing. Surface browning is the  
45 major limiting factor for the shelf-life of fresh-cut apple, and its appearance strongly

46 and negatively affects the consumer's purchase decision (Shrestha et al., 2020;  
47 Toivonen and Brummell, 2008).

48 Enzymatic browning of fresh-cut fruit and vegetable is a complex and highly  
49 regulated process. It is generally considered that polyphenol oxidase (PPO) catalyses  
50 the oxidation of phenolic compounds to quinones which then condense to form brown  
51 polymers (Milani and Hamed, 2004). In a typical plant cell PPO is associated with  
52 the plastid and phenolic substrates are located in the vacuole. Cellular and  
53 intracellular disruption by cutting allows the substrates to mix and hence react to form  
54 browning polymers (Landrigan et al., 1996). However, PPO activity and phenolic  
55 content are not the only factors affecting browning reaction. Li et al. (2017) indicated  
56 that the lipid membrane of cells may be an important factor in browning of fresh-cut  
57 pear as a higher lipoxygenase (LOX) activity, lower unsaturated fatty acid ratio and  
58 severe cell membrane damage accompanied a stronger degree of browning. Cysteine  
59 protease inhibitors inhibited the browning of fresh-cut potato through reducing the  
60 accumulation of free amino acids (Dong et al., 2020), implying that protein  
61 degradation is an integral component of the browning mechanism. After the browning  
62 of fresh-cut lotus tubers, the ROS metabolism homeostasis was damaged and energy  
63 efficiency decreased as the antioxidant enzymes (TPX and SOD) and energy  
64 metabolism related protein (H<sup>+</sup>-ATPase, PDC) were down-regulated (Jiang et al.,  
65 2012). Recent studies have used high-throughput transcriptome sequencing  
66 techniques to characterize the expression profile of the browning response in different  
67 types of fruit and vegetable after cutting. Several enzymatic browning-related  
68 differentially expressed genes are consistently implicated, including *PPO*,  
69 *phenylalanine ammonia lyase (PAL)*, *peroxidase (POD)*, *catalase (CAT)*, *superoxide*  
70 *dismutase (SOD)* (Docimo et al., 2016; Zhang et al., 2019; Zhu et al., 2017). However,

71 the transcriptomic events that occur during the browning process of fresh-cut apple is  
72 still unknown.

73 Hydrogen sulfide (H<sub>2</sub>S) is the third endogenous signaling molecule after carbon  
74 monoxide and nitric oxide, which is traditionally known as a toxic gas. In the past  
75 decade, studies showed that it can be generated in many types of mammalian cells and  
76 might be beneficial to human health via multiple mechanisms (Giovinazzo et al., 2021;  
77 Wang, 2002). In plant, H<sub>2</sub>S has been revealed not only to regulate normal  
78 physiological processes (Hancock and Whiteman, 2014; Jin and Pei, 2015), but also  
79 to prevent the postharvest senescence of fruit and vegetable (Hu et al., 2012; Hu et al.,  
80 2014a). Recent research has demonstrated H<sub>2</sub>S treatment could inhibit surface  
81 browning in many types of fresh-cut fruit and vegetable by regulating the phenolic  
82 metabolism or antioxidant defense system (Sun et al., 2015; Zheng et al., 2016). In  
83 these paper, the application concentration of H<sub>2</sub>S were quite low. Furthermore, the  
84 essential oils in organosulphur rich fruits and vegetables, such as onion, garlic, shallot,  
85 leek, can be metabolized to generate H<sub>2</sub>S in biological conditions and modulate cell  
86 signaling (Liang et al., 2015). Thus we propose that trace H<sub>2</sub>S gas used in storage and  
87 preservation of fruits and vegetables could be safe. However, the underlying  
88 molecular mechanism of browning inhibition by H<sub>2</sub>S is still unknown. In the present  
89 study, transcriptome analysis was performed using a high-throughput sequencing  
90 platform (Illumina HiSeq<sup>TM</sup>2000) to give new insights into the mechanism of  
91 browning inhibition by H<sub>2</sub>S treatment in fresh-cut apple.

92

## 93 **2. Materials and Methods**

94

## 95 2.1 Sample preparation and treatments

96

97 “Fuji” apple (*Malus domestica* cv. Red Fuji) were freshly harvested from a  
98 commercial farm in Dalian City, P. R. China in October 2017. Apples were selected  
99 based on uniform color, size, hardness, and the absence of any visible physical defects  
100 and fungal infections. After harvest, the fruit were immediately transported to the  
101 laboratory at Dalian Minzu University and stored at 4 °C prior to the experiments. In  
102 these apples, weight ( $312.9 \pm 37.4$  g), equatorial ( $9.1 \pm 0.5$  cm), longitudinal ( $8.1 \pm$   
103  $0.3$  cm) diameters were monitored. These fruits were rinsed gently by hand, using tap  
104 water, and were dried naturally. After that, apples were peeled, cored, then cut into 2  
105 cm-thick cubes with a sharp stainless-steel knife. The cubes of each apple were  
106 divided into two groups, one was used for the H<sub>2</sub>S treatment and the other one was the  
107 control. Sodium hydrosulfide (NaHS, Sigma) solutions were used as the H<sub>2</sub>S donor  
108 and 200 mL of  $0.7 \text{ mmol}\cdot\text{L}^{-1}$  NaHS was prepared and placed into the bottom of  
109 sealed containers (desiccators) which themselves had a total volume 3 L. This  
110 solution could release H<sub>2</sub>S gas into the container headspace rapidly and reached the  
111 peak concentration within 30 min, which was then maintained at a constant  
112 concentration of  $0.30 \times 10^{-10} \text{ mol}\cdot\text{L}^{-1}$  H<sub>2</sub>S gas for the duration of sample treatment (Hu  
113 et al., 2012). Fresh-cut apple were placed on a grid above the NaHS solution and  
114 thereby exposed to H<sub>2</sub>S treatment for 24 h. Water was used instead of NaHS solution  
115 in the control samples. Three independent containers were set up to generate H<sub>2</sub>S and  
116 likewise there were three independent control samples. After treatment, samples were  
117 placed in a different plastic box ( $15 \times 21 \times 2.5$  cm) for each replicate and each box  
118 was wrapped with polyethylene cling film to prevent further gas exchange. The time

119 when the control and H<sub>2</sub>S treatment ended was defined as day 0 and from this time  
120 point on, all samples were stored for up to 12 d at 4 ± 1 °C.

121

## 122 2.2 Measurement of color

123

124 The color of fresh-cut apple was measured every two days using repeated  
125 measures of eight fresh cut apple cubes. Color data were captured using a Minolta  
126 Chroma Meter Model CR-300 (Minolta. Tokyo, Japan), using the CIELAB color  
127 parameters, *L\** (lightness), *a\** (green chromaticity) and *b\** (yellow chromaticity).  
128 Browning index (BI) was calculated as follows (Palou et al., 1999):

$$129 \quad BI = [100(x-0.31)]/0.172$$

130 where  $x = (a^*+1.75L^*)/(5.645L^*+a^*-3.012b^*)$

131

## 132 2.3 Enzyme activities

133

134 All enzyme extracts were prepared by homogenizing 5 g of fresh-cut apple in a  
135 homogenizer (T-25, IKA, Germany), on ice, using the following extraction media: 20  
136 mL of 0.2 mol L<sup>-1</sup> phosphate buffer (pH 6.4) containing 0.1 g  
137 polyvinylpolypyrrolidone (PVPP) for PPO, POD, SOD, CAT, glutathione reductase  
138 (GR) and 20 mL of 0.1 mol L<sup>-1</sup> phosphate buffer (pH 7.5) containing 1 mmol L<sup>-1</sup>  
139 ethylenediaminetetraacetic acid (EDTA) and 3 mmol L<sup>-1</sup> ascorbic acid for ascorbate  
140 peroxidase (APX). For phenylalanine ammonia lyase (PAL): the extraction solution  
141 was 20 mL of 0.1 mol L<sup>-1</sup> sodium borate buffer (pH 8.7) containing 0.037 % EDTA,  
142 0.137 % β-mercaptoethanol and 3 % PVPP. Extracts were then centrifuged at 12 000  
143 g, for 30 min, at 4 °C, and supernatants were collected for further analysis.



144 PPO and POD activities were examined using the method reported by Chen et al.  
145 (2016a). One unit of PPO and POD activities was defined as a decrease of OD value  
146 in absorbance per minute.

147 PAL activity was measured by using a method reported by Yin et al. (2012). One  
148 unit of PAL activity was defined as a decrease of  $0.01 \times$  OD value in absorbance per  
149 minute.

150 SOD activity was measured using p-nitro-blue tetrazolium chloride (NBT)  
151 according to Ren et al. (2012). One unit of SOD activity was defined as the amount of  
152 enzyme that caused 50 % inhibition of NBT.

153 CAT activity was determined according to Ren et al. (2012), by monitoring the  
154 disappearance of  $H_2O_2$  by recording the decrease in absorbance at 240 nm. One unit  
155 of CAT activity was defined as a decrease of  $0.01 \times$  OD value in absorbance per  
156 minute.

157 APX activity was measured by determining the amount of oxidized ascorbate  
158 using the method of Ren et al. (2012). One unit of APX activity was defined as a  
159 decrease in the OD value in absorbance per minute.

160 GR activity was examined based on the oxidation of nicotinamide-adenine  
161 dinucleotide phosphate (NADPH) and the change of absorbance at 340 nm was  
162 monitored (Zhang et al., 2017). One unit of GR activity was defined as the amount of  
163 enzyme that oxidized 1  $\mu$ mol NADPH per min.

164 All the enzymatic activities were expressed as  $U\ kg^{-1}\ FW$ .

165

166 2.4  $H_2O_2$  content

167

168 Three grams of fresh-cut apple were put into 5 mL of cold acetone (100 %) and

169 then homogenized. Subsequently, the mixture was centrifuged (Allegra X-30R,  
170 Beckman Coulter, USA) for 20 min (10000 g, 4 °C). The supernatant was used to  
171 analyze H<sub>2</sub>O<sub>2</sub> content by the titanium peroxide method (Patterson et al., 1984). The  
172 result was expressed as mmol kg<sup>-1</sup>. There were three independent biological replicates  
173 for the control and the H<sub>2</sub>S treatment.

174

#### 175 2.5 Ascorbic acid content

176

177 Ascorbic acid (AsA) content was determined according to AOAC (1990) by  
178 using titration with 2,6-dichlorophenolindophenol. The result was calculated by  
179 comparison to a standard AsA curve and expressed in mg of AsA per kg fresh weight.  
180 There were three independent biological replicates for the control and the H<sub>2</sub>S  
181 treatment.

182

#### 183 2.6 Phenolic content

184

185 Phenolic compounds were extracted into 75 % ethanol and the content of  
186 individual phenolics was determined by using an Agilent Technologies (Waldbronn,  
187 Germany) 1100 Series HPLC system according to Chen et al. (2016b). Ten µL of  
188 each sample was filtered and then separated using a Hypersil BDS C18 column (250  
189 mm × 4.6 mm, 5 µm; Thermo, Bellefonte, PA, USA). The phenolics were eluted by  
190 using two mobile phases (A: 2 % v/v acetic acid in water, B: 2 % v/v acetic acid in  
191 water and acetonitrile, 50:50, v/v) with a linear gradient from 10 to 55 % B in 50 min  
192 and monitored at 254 nm (for quercetin, eugenol, epicatechin), 280 nm (for catechin,  
193 tannic acid, vanillic acid) and 320 nm (for caffeic acid and chlorogenic acid). The

194 flow rate was 1 mL min<sup>-1</sup>. The result was calculated by comparison to standard curves  
195 constructed from dilutions of pure standards for each phenolic compound and  
196 expressed as mg per kg of sample.

197

## 198 2.7 Transcriptome Analysis

199

### 200 2.7.1 mRNA library construction and sequencing

201 Total RNA was extracted from each biological replicate of the control and H<sub>2</sub>S  
202 treatment using Trizol reagent (Invitrogen, CA, USA) following the manufacturer's  
203 procedure. The total RNA quantity and purity were analysed using a Bioanalyzer  
204 2100 and RNA 6000 Nano LabChip Kit (Agilent, CA, USA) with RIN number >7.0.  
205 Approximately 10 µg of total RNA representing a specific adipose type was subjected  
206 to isolation of Poly (A) mRNA with poly-T oligo attached magnetic beads  
207 (Invitrogen). Following purification, the mRNA was fragmented into small pieces  
208 using divalent cations under elevated temperature. Then the cleaved RNA fragments  
209 were reverse-transcribed to create the final cDNA library in accordance with the  
210 protocol for the mRNA Seq sample preparation kit (Illumina, San Diego, USA), the  
211 average insert size for the paired-end libraries was 300 bp (±50 bp). We then  
212 performed the paired-end sequencing on an IlluminaHiseq4000 at the LC Sciences  
213 (Hangzhou, Zhejiang, China), following the vendor's recommended protocol.

214

### 215 2.7.2 RNA-seq reads mapping

216 The clean reads were mapped onto the apple genome GDDH13 Version 1.1  
217 (<https://iris.angers.inra.fr/gddh13/the-apple-genome-downloads.html>) using HISAT  
218 (Johns Hopkins University Center for Computational Biology, Baltimore, MD, USA).

219 <https://daehwankimlab.github.io/hisat2/>,version:hisat2-2.0.4), which initially removed  
220 a portion of the reads based on quality information accompanying each read and then  
221 mapped the reads to the reference genome (Kim et al., 2015). HISAT allows multiple  
222 alignments pre-read (up to 20 by default) and a maximum of two mismatches when  
223 mapping the reads to the reference. HISAT build a database of potential splice  
224 junctions and confirms these by comparing the previously unmapped reads against the  
225 database of putative junctions.

226

### 227 2.7.3 Transcript abundance estimation and differentially expressed testing

228 The mapped reads of each sample were assembled using StringTie  
229 (<http://ccb.jhu.edu/software/stringtie/>,version:stringtie-1.3.4d.Linux\_x86\_64, Pertea et  
230 al., 2015) with default parameters (command line: `~stringtie -p 4 -G genome.gtf -o`  
231 `output.gtf -l sample input.bam`). Then, all transcriptomes from samples were merged  
232 to reconstruct a comprehensive transcriptome using perl scripts. After the final  
233 transcriptome was generated, StringTie and Ballgown  
234 (<http://www.bioconductor.org/packages/release/bioc/html/ballgown.html>) was used to  
235 estimate the expression levels of all transcripts (Frazee et al., 2015; Pertea et al.,  
236 2015). StringTie was used to perform expression level for mRNAs by calculating  
237 FPKM. The differentially expressed mRNAs and genes were selected with  $|\log_2FC| \geq$   
238 1 and with statistical significance ( $P < 0.05$ ) by R package-Ballgown

239

### 240 2.8 Quantitative Real-Time PCR (qRT-PCR)

241

242 To validate the RNA-Seq data, the expression of 10 selected DEGs were  
243 quantified by using qRT-PCR following the manufacturer's protocols (One Step

244 SYBR<sup>®</sup> PrimeScript<sup>™</sup> RT-PCR Kit, TaKaRa, Japan). Total RNA was extracted from  
245 three independent biological replicates of both the control and H<sub>2</sub>S treated apple  
246 material and purified by using TaKaRa MiniBEST Plant RNA Extraction Kit  
247 (TaKaRa, Japan). The sequences of gene specific qRT-PCR primers are listed in  
248 Supplementary Table S1. *Md18sRNA* was used as a housekeeping gene. Calculation  
249 of the relative quantification was performed by the comparative 2<sup>- $\Delta\Delta$ CT</sup> method (Livak  
250 and Schmittgen, 2001). Three biological replicates were used for qRT-PCR analysis.

251

### 252 **3. Results and discussion**

253

#### 254 3.1 Effect of H<sub>2</sub>S treatment on the browning of fresh-cut apple

255

256 Surface browning is one of the major limiting factors for the shelf life of  
257 fresh-cut apple and strongly and negatively affects the consumers' decision whether or  
258 not to purchase the product. As shown in Fig. 1A, the initial surface color of  
259 H<sub>2</sub>S-treated fresh-cut apple was a clean, pale yellow. The control samples had already  
260 started to discolor from the time spent in the incubator post-cutting. As the storage  
261 time progressed, the color of control samples turned to a pale brown. H<sub>2</sub>S treatment  
262 effectively inhibited the surface browning of fresh-cut apple over the 12 d of storage,  
263 with discoloration remaining less than the browning index (BI) of the control at day 0  
264 throughout the experiment. The BI refers to the intensity of the brown color and has  
265 been considered an important indicator of the browning degree. A continual increase  
266 in BI of fresh-cut apple was observed during storage (Fig. 1B). H<sub>2</sub>S treatment clearly  
267 suppressed the increase in browning degree over the entire storage period.

268

## 269 3.2 Physiological responses of fresh-cut apple to H<sub>2</sub>S treatment

270

271 To assess the physiological responses of fresh-cut apple to H<sub>2</sub>S treatment, we  
272 monitored the activities of PPO, POD, PAL, SOD, CAT, APX and GR, the contents of  
273 H<sub>2</sub>O<sub>2</sub>, AsA and phenolics during storage at 4 °C (Fig. 2). H<sub>2</sub>S treatment significantly  
274 increased the enzyme activities of SOD, CAT, GR, PAL and increased the contents of  
275 AsA and phenolics, whilst it inhibited the accumulation of H<sub>2</sub>O<sub>2</sub> and PPO, POD and  
276 APX activities, as compared with the control ( $P < 0.05$ ). It is interesting to note that  
277 the activities of five enzymes (PPO, PAL, CAT, SOD and APX) reached their  
278 maximum or minimum on the 6th day of storage. Therefore, fresh-cut apple samples  
279 that were taken immediately after H<sub>2</sub>S treatment (day 0) and after storage at 4 °C for 6  
280 d were used for transcriptome analysis to explore the molecular mechanism of  
281 browning inhibition.

282

## 283 3.3 Transcriptome gene expression analysis

284

285 In order to investigate the molecular mechanism initiated by H<sub>2</sub>S treatment in  
286 browning inhibition of fresh-cut apple, RNA-Seq libraries were designed including  
287 control and H<sub>2</sub>S treated samples at two stage (day 0 and day 6). Supplementary Table  
288 S2 and S3 provide a quality summary of the sequence data and the number of unigene  
289 and transcript identified in each sample. There were 21, 26, 6 and 12 uniquely  
290 expressed genes were found in C0, S0, C6 and S6, respectively (Table S4). We totally  
291 identified 3782 (1638 up-regulated and 2144 down-regulated) and 1164 DEGs (529  
292 up-regulated and 635 down-regulated) in S0 vs. C0 and S6 vs. C6, respectively, only  
293 406 genes in common (Fig. 3A, 3B). There are more DEGs in S0 vs. C0 than that in

294 S6 vs. C6, indicating that a majority of transcriptional responses were manifested  
295 soon after the treatments. The top up-regulated DEG in S0 vs. C0 and S6 vs. C6 were  
296 *zinc finger AN1 domain-containing stress-associated protein 12* and *glutathione*  
297 *S-transferase (GST)*, respectively. *Polygalacturonase inhibitor 2* was the top  
298 down-regulated DEG in both S0 vs. C0 and S6 vs. C6 (Table S5). Then we analyze  
299 the possible browning-related genes in the DEGs of two samples. In the control, there  
300 were 775 and 879 DEGs up- and down-regulated respectively at day 6 relative to day  
301 0. While in the H<sub>2</sub>S treatment, 1171 and 1144 DEGs up- and down-regulated were  
302 identified respectively after 6 d storage, only 312 were in common (Fig, 3C). This  
303 limited overlap in transcriptomic events indicating that H<sub>2</sub>S treatment altered the gene  
304 expression patterns of fresh-cut apple during storage and this change might be related  
305 to the browning inhibition.

306 GO term enrichment analyses were conducted for DEGs in S0 vs. C0, S6 vs. C6,  
307 C6 vs. C0 and S6 vs. S0, respectively, to evaluate the potential functions of these  
308 genes. The top 15 enriched GO terms ( $P < 0.05$ ) of biological process, cellular  
309 component and molecular function are shown in Fig. 4A-D. When comparing the GO  
310 terms in S0 vs. C0 to S6 vs. C6, 18 out of 45 GO term were found in common. Within  
311 the biological process category, “oxidation-reduction process” was the most enriched  
312 term in both S0 vs. C0 and S6 vs. C6. Besides, several GO terms related to response to  
313 abiotic stresses, such as salt stress, cold, heat, water deprivation, were significantly  
314 enriched in both two comparable pairs. For cellular component, GO terms related to  
315 membrane, such as “plasma membrane”, “integral component of plasma membrane”,  
316 “vacuolar membrane”, dominated in both S0 vs. C0 and S6 vs. C6. In S0 vs. C0,  
317 DEGs associated with “transferase activity” was the most dominated GO term in  
318 molecular function, while that was “metal ion binding” in S6 vs. C6. There were five

319 common GO terms in S0 vs. C0 and S6 vs. C6, including genes coding proteins with  
320 “oxidoreductase”, “glutathione transferase activity”, “pyridoxal phosphate binding”  
321 etc.

322 Next, we compared the function of DEGs in C6 vs. C0 and S6 vs. S0, only 11  
323 GO terms were found in common, indicating that H<sub>2</sub>S treatment changed the  
324 metabolism of fresh-cut apple, which might be involved in the browning inhibition  
325 (Fig 4C, 4D). For biological process, the most dominated GO term was  
326 “oxidation-reduction process” in the control, while that was “protein ubiquitination”  
327 in the H<sub>2</sub>S treatment. Six common GO terms were found in C6 vs. C0 and S6 vs. S0.  
328 Within the cellular component category, “cytoplasm”, “integral component of plasma  
329 membrane” and “nuclear speck” were significantly enriched in both control and H<sub>2</sub>S  
330 treatment. “cytoplasm” was the most dominated GO terms in the control, which was  
331 the second enriched GO terms in the H<sub>2</sub>S treatment. The largest group number of  
332 DEGs in the H<sub>2</sub>S treatment were enriched in “nucleus”. Besides, several GO terms  
333 related to membrane, such as “plasma membrane”, “vacuolar membrane”,  
334 “endoplasmic reticulum membrane”, “Golgi membrane” and “endosome membrane”  
335 were only enriched in the H<sub>2</sub>S treatment. The top three GO terms for molecular  
336 function in the control and H<sub>2</sub>S treatment were “nucleic acid binding”,  
337 “oxidoreductase activity” “ubiquitin-protein transferase activity” and “protein  
338 serine/threonine kinase activity”, “nucleotide binding”, “transferase activity”,  
339 respectively. To further understand the changes induced by H<sub>2</sub>S related to the  
340 browning process, the gene expression pattern of DEGs in the control and H<sub>2</sub>S  
341 treatment within the common GO terms were analyzed (Fig. S1). H<sub>2</sub>S treatment  
342 increased the number of up-regulated DEGs in “glucose import” and “glucose  
343 transmembrane transporter activity”, while increased the down-regulated DEGs in



344 “integral component of plasma membrane”, “lipid metabolic process”, “negative  
345 regulation of transcription”, “protein ubiquitination” and “response to cold”.  
346 Therefore, these DEGs expression pattern changes together with the involvement of  
347 “membrane”, “nucleus” induced by H<sub>2</sub>S might be related to the browning inhibition.

348 In order to characterize the pathways that related to the browning inhibition by  
349 H<sub>2</sub>S treatment, we performed pathway enrichment analysis on DEGs based on the  
350 KEGG database with  $P < 0.05$  as the threshold. We found that 25/102, 11/98, 11/125  
351 and 6/123 pathways demonstrated significant changes in S0 vs.C0, S6 vs. C6, C6 vs.  
352 C0 and S6 vs. S0, respectively (Table S6). There were seven pathways that were all  
353 enriched in the H<sub>2</sub>S treatment versus the control at both stages of shelf life, including  
354 two within carbohydrate metabolism and two representing lipid metabolism. The  
355 pathways that were specifically enriched in S0 vs.C0 included five of carbohydrate  
356 metabolism and six of amino acid metabolism. However, three pathways representing  
357 biosynthesis of secondary metabolites (phenylpropanoid biosynthesis, flavonoid  
358 biosynthesis and anthocyanin biosynthesis) were only found in S6 vs. C6. Two  
359 pathways “Circadian rhythm-plant” and “Biotin metabolism” were found in both  
360 control and H<sub>2</sub>S treatment during storage. “Ubiquitin mediated proteolysis” had the  
361 largest number of DEGs in S6 vs. S0.

362

### 363 3.4 Differentially expressed genes related to phenol peroxidases and phenolics

364

365 Surface browning of fresh-cut products results from the oxidation of phenolic  
366 substances to quinones catalyzed by phenol oxidases (such as PPO and/or POD),  
367 which subsequently condense to form browning polymers (Degl'Innocenti et al., 2005;  
368 Saltveit, 2000). Suppression of *PPO* genes was an effective approach to reduce the

369 browning of potato tuber (Chi et al., 2014; Coetzer et al., 2001). In the same way,  
370 numerous studies have shown that the inhibition of surface browning of fresh-cut  
371 apple was accompanied by a decrease in PPO activity (Hemachandran et al., 2017;  
372 Saba and Sogvar, 2016). In the present study, one gene encoding PPO was  
373 up-regulated (*MSTRG.17066*, a 1.72 log<sub>2</sub>FC significant increase) in the control at day  
374 6 relative to day 0, but no significant change in *PPO* expression was observed in H<sub>2</sub>S  
375 treatment during storage (Fig. 5). H<sub>2</sub>S treatment showed significant reductions in gene  
376 expression of *PPO* relative to the control at day 0 (*MSTRG.17063*, a 2.2 log<sub>2</sub>FC  
377 significant reduction) and day 6 (*MSTRG.9035*, a 1.9 log<sub>2</sub>FC significant reduction).  
378 This result fits with the observed pattern of PPO activity of fresh-cut apple (Fig. 2).  
379 The PPO activity in the control samples at day 6 was higher than that at day 0 and  
380 H<sub>2</sub>S treated samples showed consistently lower PPO activity than the control.

381 The POD enzyme, which uses H<sub>2</sub>O<sub>2</sub> as a catalyst for the oxidation of phenolic  
382 compounds (Reyes et al., 2007), could also enhance browning reactions in the  
383 presence of ongoing PPO-mediated browning (Richard-Forget and Gauillard, 1997).  
384 In the present study, two *POD* genes (*MSTRG.11943*, *MSTRG.22268*) were induced,  
385 while one *POD* (*MSTRG.27890*) was repressed by H<sub>2</sub>S treatment. *MSTRG.22268* was  
386 up-regulated and *MSTRG.27890* was down-regulated in the control at day 6 relative to  
387 day 0, but they did not differentially expressed in the H<sub>2</sub>S treatment during storage.  
388 *MSTRG.11943* was down-regulated in the H<sub>2</sub>S treatment but was not differentially  
389 expressed in the control during storage. Three genes encoding POD (*MSTRG.28170*,  
390 *MSTRG.6438*, *MSTRG.898*) were repressed in S6 vs. C6. Only *MSTRG.6438* was  
391 found differentially expressed in both control (a 2.11 log<sub>2</sub>FC significant increase) and  
392 H<sub>2</sub>S treatment (a 1.78 log<sub>2</sub>FC significant increase) during storage (Fig. 5). Therefore,  
393 H<sub>2</sub>S treatment was effective at repressing induction of *MSTRG.6438* that would

394 normally be expressed at a later stage post-cutting, which might be related to the  
395 browning inhibition. It is unclear why fresh-cut apple has different copies of POD  
396 genes and showed different expression patterns in H<sub>2</sub>S treatment relative to the  
397 control at two stages. We speculated that the cutting process induced the production of  
398 ROS, but H<sub>2</sub>S treatment stopped the induction of the POD that would normally use  
399 H<sub>2</sub>O<sub>2</sub> as a catalyst for oxidation of phenolic compounds. Six-day storage led to  
400 accumulation of ROS in control tissues, providing a higher concentration of H<sub>2</sub>O<sub>2</sub> and  
401 enabling significant levels of POD-mediated polyphenol browning. However, H<sub>2</sub>S  
402 treatment was not able to completely inhibit either the expression of *POD* genes or the  
403 enzymic activity of POD. There is also a debate on the correlation between POD  
404 activity and browning reactions of fresh-cut fruit and vegetable in previous reports  
405 (Liu et al., 2019; Sun et al., 2015) and leads to the conclusion that the function of the  
406 *POD* gene family needs to be further studied.

407 The biosynthesis of phenolics, which are the substrates of enzymatic browning  
408 reactions, involves a complex network of routes based on the shikimate and  
409 phenylpropanoid pathways. Genes encoding chorismate mutase (CM), chorismate  
410 synthase (CS), PAL and shikimate O-hydroxycinnamoyltransferase (HCT), which  
411 involved in the shikimic acid pathway and subsequent conversion of chorismate to  
412 phenylalanine, and phenylpropanoid pathways were all up-regulated in S0 vs. C0 or  
413 S6 vs. C0, while *bifunctional 3-dehydroquininate dehydratase/shikimate dehydrogenase*  
414 (*3DD, SD*), *4-coumarate-CoA ligase (4CL)*, were down-regulated. The implication of  
415 these findings is that H<sub>2</sub>S treatment actually induces the synthesis of phenolic  
416 compounds and this is further supported by the biochemical assays which  
417 demonstrated the significantly higher accumulation of several phenolic compounds  
418 (chlorogenic acid, vanillic acid, catechin, tannic acid, quercetin), in H<sub>2</sub>S treated

419 samples compared to the control during the storage. Chlorogenic acid and catechin  
420 were reported to be good substrates for PPO in apple (Amaki et al., 2011). Therefore,  
421 we concluded that H<sub>2</sub>S mediated delay of browning of fresh-cut apple is not through  
422 reduction of the phenolic substrates.

423

### 424 3.5 Differentially expressed genes related to lipid metabolism

425

426 Although the eventual browning symptoms occur because of the interactions  
427 between PPO and/or POD enzymes and phenolic substrates, the enzymes and  
428 substrates are ordinarily separated from each other by intracellular membranes.  
429 Docimo et al. (2016) has reported that there was a lack of correlation between flesh  
430 browning and PPO activity or phenolic content in cut eggplant. Similarly, Cantos et  
431 al. (2002) has found that PPO activity and phenolic compounds are not rate-limiting  
432 in browning development of fresh-cut potatoes. Li et al. (2017) has reported that the  
433 membrane may be an important factor in browning of fresh-cut pear and the  
434 browning was caused by the cell membrane degradation which damaged the cell  
435 compartmentalization. Therefore, the progress of the browning reaction was thought  
436 to be related to the processes that affect the membrane integrity. Besides the loss of  
437 cell integrity due to processing, the breakdown of membranes within cells of fruit  
438 tissues during storage also causes the loss of cellular compartmentalization, and  
439 subsequently increases the degree of browning (Toivonen and Brummell, 2008, Li et  
440 al., 2017). Since lipids are essential constituents of the cell membrane, any alteration  
441 of membrane lipid composition such as the decrease of unsaturated fatty acids, the  
442 increase of saturated fatty acids, or degradation of membrane phospholipids, may  
443 change the biophysical and/or biochemical membrane properties and damage the

444 integrity of membrane (Saquet et al., 2003; Zhang et al., 2018)). In the present study,  
445 of the 13 DEGs related to the fatty acid metabolism in the control samples, three  
446 were up-regulated at day 6 compared to day 0, whereas ten were down-regulated  
447 over the same storage period. With the addition of H<sub>2</sub>S treatment, 12 genes were  
448 differentially expressed, with ten up-regulated at day 6 compared to day 0, and two  
449 down-regulated over the same storage period. Among the DEGs in the control and  
450 H<sub>2</sub>S treatment during storage, only two genes were in common, which were  
451 up-regulated in both samples. Comparing the DEGs in H<sub>2</sub>S treatment to the control  
452 found that most genes (19 out of 21) were down-regulated at day 0, but three out of  
453 four genes were up-regulated at day 6 (Table S7). Glycerophospholipid metabolism  
454 also changed after H<sub>2</sub>S treatment, 11 (six genes were up-regulated and five genes  
455 were down-regulated) and 20 DEGs (eight genes were up-regulated and 12 genes  
456 were down-regulated) were found in the control and H<sub>2</sub>S treatment at day 6 relative  
457 to day 0, respectively. There were 37 and 10 genes differentially expressed in S0 vs.  
458 C0 and S6 vs. C6, respectively (Table S8).

459 LOX and PLD are two important lipids-degrading enzymes, which induce the  
460 degradation of unsaturated fatty acids and phospholipids, respectively. Mellidou et al.  
461 (2014) revealed that the expression of genes encoding LOX and PLD increased when  
462 browning developed during the storage of apple. In the present study, we did not find  
463 the same result as the literature shown, one *LOX* and one *PLD* were down-regulated  
464 in the control at day 6 relative to day 0, which was not differentially expressed in the  
465 H<sub>2</sub>S treatment during storage. But comparing the H<sub>2</sub>S treatment to the control, three  
466 genes encoding PLD and two genes encoding LOX were down-regulated at day 0 and  
467 two of these *PLDs* and one *LOX* maintained low expression by day 6 of storage (Fig.  
468 5). The down-regulation of these genes might increase the content of unsaturated fatty

469 acids and phospholipids in H<sub>2</sub>S treated material, thus retarding the damage of cellular  
470 membrane structure that would otherwise occur in the control. H<sub>2</sub>S treatment reduced  
471 LOX activity and lipid peroxidation has also been observed in other fresh-cut fruit  
472 (Gao et al., 2013; Zheng et al., 2016). It can thus be suggested that H<sub>2</sub>S treatment  
473 could suppress the activation of membrane lipids-degrading enzymes, possibly at a  
474 level of transcriptional regulation by inhibiting the expression of genes *LOX* and *PLD*,  
475 which in turn might retard the degradation of cell membrane lipids and maintain the  
476 integrity of cell membrane structure.

477

### 478 3.6 Differentially expressed genes related to antioxidant systems

479

480 Mechanical injury by cutting processing increased the production of reactive  
481 oxygen species (ROS), which induce membrane lipid peroxidation and promote  
482 browning reactions. Antioxidant enzymes and antioxidants inside the fruit tissues are  
483 necessary for ROS detoxification (Møller, 2001). Enhancing enzymatic and  
484 non-enzymatic antioxidant capacities to alleviate the oxidative damage is one way to  
485 inhibit the browning of fresh-cut fruit and vegetable during storage (Hu et al., 2014b;  
486 Zheng et al., 2016). H<sub>2</sub>S treatment induced the expression of genes encoding GST, as  
487 16 and 6 *GSTs* were found up-regulated in H<sub>2</sub>S treatment relative to the control at day  
488 0 and day 6, respectively. Six and two *GSTs* were up-regulated and down-regulated in  
489 the control at day 6 relative to day 0, respectively. Seven of these genes remained  
490 unchanged in the H<sub>2</sub>S treated samples over the same storage period, but five detected  
491 *GSTs* in the H<sub>2</sub>S treatment were all down-regulated. These results indicated that H<sub>2</sub>S  
492 treatment activated the GSTs expression at an earlier stage, but most of them have less  
493 longevity (Fig. 5). Besides, one gene encoding CAT and one gene encoding SOD all

494 showed significantly higher expression, while two *APXs* showed significantly lower  
495 expression in tissue from the H<sub>2</sub>S treatment compared to control at day 0.  
496 Physiological results supports this, the activities of SOD and CAT increased while  
497 APX activity decreased after H<sub>2</sub>S treatment (Fig. 2). After 6 d of storage, only one  
498 APX-encoding gene was up-regulated, whilst one gene encoding APX and one  
499 encoding SOD were down-regulated in H<sub>2</sub>S treatment relative to the control. There  
500 were three and two *SODs* down-regulated in the control and H<sub>2</sub>S treatment,  
501 respectively. Therefore, it is reasonable to see that the number of up-regulated DEGs  
502 involved in antioxidant systems was greater in S0 vs. C0 compared to those in S6 vs.  
503 C6 (Fig. 5), implying that the antioxidant capacities of H<sub>2</sub>S treated sample at day 0  
504 were higher than at day 6.

505 AsA is an antioxidant that is able to interact with ROS directly or together with  
506 antioxidant enzymes. AsA plays an important role in the development of browning.  
507 Exogenous application of AsA effectively inhibited the browning of fresh-cut fruit  
508 (Yan et al., 2017) and browning does not occur unless the endogenous AsA  
509 concentration falls below a certain threshold value (Franck et al., 2007). In the plant  
510 cell, AsA can be continuously oxidized through enzymatic (*APX* and *AO*) or  
511 non-enzymatic reactions and can be reduced back to AsA by recycling reductases  
512 (*DHAR*, *MDHAR*) (Cocetta et al., 2014). The AsA recycling pathway has been  
513 evidenced as important for the re-establishment of AsA in horticultural crops  
514 (Mellidou and Kanellis, 2007). Although *APX* in fresh-cut apple was down-regulated  
515 in S0 vs. C0, the expression of *AO* and *MDHAR* was up-regulated in S0 vs. C0, while  
516 they were unchanged after 6 d of storage. In the control sample, one *AO* was  
517 up-regulated at day 6 relative to day 0, but three *AOs* were down-regulated and two  
518 *MDHARs* were up-regulated in the H<sub>2</sub>S treatment during storage (Fig. 5). This result

519 suggested that AsA recycling pathway was triggered by H<sub>2</sub>S, but it did not work  
520 efficiently after storage. The transcriptome results corresponded well to the content of  
521 AsA. We observed a decrease of AsA in fresh-cut apple during storage, regardless of  
522 treatment, but H<sub>2</sub>S treatment significantly inhibited the decline. Overall, the  
523 up-regulation of antioxidant enzymes and AsA recycling-related gene expression  
524 aided ROS scavenging, as we observed that H<sub>2</sub>S significantly alleviated the  
525 accumulation of H<sub>2</sub>O<sub>2</sub> and maintained it at a lower level compared with the control  
526 throughout storage. The ability of H<sub>2</sub>S treatment to increase the antioxidant capacity  
527 and reduce the accumulation of ROS has also been reported in various fresh-cut fruit  
528 and vegetable (Sun et al., 2015; Zheng et al., 2016). Therefore, we concluded that H<sub>2</sub>S  
529 treatment delayed browning of fresh-cut apple might be associated with its effect on  
530 enhancing the antioxidant defense capacity, which reduced the oxidative damage from  
531 ROS.

532

### 533 3.7 Differentially expressed genes related to energy metabolism

534

535 An increasing body of evidence has demonstrated that the browning of  
536 postharvest horticultural crops is often accompanied by lower levels of ATP content  
537 and energy charge (Franck et al., 2007; Lin et al., 2018). ATP, as an "energy flux",  
538 plays an important role in lipid synthesis and cell membrane restoration. Once ATP  
539 production rate is lower than a certain threshold, free fatty acids will be released from  
540 phospholipids and the cell membrane structure will be damaged (Rawyler et al., 1999),  
541 which allows PPO to mix with phenolics and react to produce browning compounds.  
542 Furthermore, ATP also plays an important role in AsA cycling. ATP deficiency can  
543 lead to ROS accumulation, which resulted in membrane lipid peroxidation and the



544 membrane structural disruption. Adequate ATP is beneficial to inhibit flesh and peel  
545 browning of fruit (Saquet et al., 2003). In postharvest fruit, ATP is mainly generated  
546 by oxidative phosphorylation. In our work, 62.5% of DEGs related to oxidative  
547 phosphorylation were down-regulated in the control at day 6 relative to day 0.  
548 However, in H<sub>2</sub>S treatment, that percent of down-regulated DEGs was reduced to  
549 31.8% (Table S9), indicating that H<sub>2</sub>S treatment retained oxidative phosphorylation  
550 capacity, which might be related to promoting browning inhibition. ATPase and NAD  
551 are key enzymes for oxidative phosphorylation (Wang et al., 2018). Jiang et al. (2012)  
552 has reported ATPase was down-regulated after fresh-cut lotus tissue browning.  
553 Transcript levels of the genes encoding the *PhATPase*  $\gamma$  and *PhATPase*  $\alpha$  subunits  
554 decreased during *Phalaenopsis* explant browning (Xu et al., 2015). Seven genes  
555 encoding ATPase (include calcium-transporting ATPase, copper-transporting ATPase  
556 etc.) and three genes encoding NAD were induced after H<sub>2</sub>S treatment (S0 vs. C0).  
557 With the prolonged storage time, the energy production capacity was gradually  
558 reduced. However, the expression of two *ATPase* and one *NAD* gene remained  
559 up-regulated in H<sub>2</sub>S treated tissue relative to control after six days of storage (Fig. 5).  
560 Therefore, the up-regulation of these genes encoding energy metabolism enzymes  
561 involved in oxidative phosphorylation by H<sub>2</sub>S treatment might increase the synthesis  
562 of ATP and thus provide enough energy for maintaining the cell membrane structure  
563 of fresh-cut apple.

564 The respiratory pathways, such as glycolysis, tricarboxylic acid (TCA) cycle,  
565 mitochondrial electron transport chain (ETC) also supply energy to maintain normal  
566 metabolism in postharvest fruit and vegetables. Most DEGs related to the respiratory  
567 pathway were down-regulated in the control fresh-cut apple during storage, while in  
568 the H<sub>2</sub>S treated sample, the number of up-regulated DEGs in glycolysis and TCA

569 increased (Table S10 and Table S11). H<sub>2</sub>S treatment therefore appears to promote the  
570 retention of metabolic processes linked to energy generation in stored fresh-cut apple.  
571 At day 0, H<sub>2</sub>S treatment induced the expression of genes encoding sucrose synthase  
572 (*SUS*) while it repressed the expression of genes encoding fructokinase as compared  
573 to the control (Fig. 5). It is suggested that *SUS* was used to cleave sucrose to provide  
574 hexose-phosphates instead of using hexokinases, which is an ATP consuming process.  
575 This alteration could save energy by using only one molecule of PPi instead of two  
576 molecules of ATP (Boeckx et al., 2019). Three genes encoding  
577 6-phosphofructokinase, one of the rate-limiting enzymes in glycolysis, were  
578 up-regulated by H<sub>2</sub>S treatment. Aldehyde dehydrogenase genes, which encode a  
579 critical enzyme for anaerobic respiration, were repressed by H<sub>2</sub>S treatment. Thus, we  
580 propose that H<sub>2</sub>S regulated glycolysis provides substrate for ATP production, rather  
581 than being consumed by anaerobic respiration. In the TCA cycle most of the DEGs  
582 (13/15) were down-regulated in S0 vs. C0, indicating that TCA pathway of fresh-cut  
583 apple was repressed by H<sub>2</sub>S treatment (Table S11). Furthermore, genes encoding  
584 mitochondrial respiratory chain complex I, II and III were induced in S0 vs. C0 or S6  
585 vs. C6 (Fig. 5), which might be expected to result in the elevated synthesis of  
586 energy-generating molecules. It is worth noting that excessive respiration would also  
587 consume metabolic substances and lead to aging and senescence. Therefore,  
588 maintaining proper respiration intensity and simultaneously supplying sufficient  
589 energy play important roles in the inhibition of browning. It can be assumed that  
590 H<sub>2</sub>S-inhibited browning of fresh-cut apple could be related to the reduction of  
591 respiratory intensity via conserving higher levels of energy in the form of ATP. This  
592 was supported by the previous reports, which confirmed that exogenous H<sub>2</sub>S  
593 treatment significantly reduced respiration rates whilst concomitantly inducing higher

594 energy production (Hu et al., 2012).

595

### 596 3.8 Validation of RNA-Seq by qRT-PCR

597

598 A total of 10 genes with differing expression patterns were selected to validate  
599 the RNA-Seq data by qRT-PCR evaluation using specific primers (Table S1). As  
600 shown in Fig. 6, correlation analysis of the gene expression ratios showed a good  
601 correlation ( $R^2 = 0.92886$ ) between qRT-PCR and RNASeq, indicating the high  
602 reliability of the RNA-Seq data obtained in our study.

603

## 604 4. Conclusions

605 Surface browning, induced by mechanical damage, is a complex and highly  
606 regulated process. H<sub>2</sub>S treatment effectively inhibited surface browning and  
607 maintained the initial color of fresh-cut apple during the storage. Transcriptome  
608 analysis revealed that the browning inhibition by H<sub>2</sub>S was mainly related to the  
609 regulation of lipid metabolism, antioxidant system, and energy metabolism. The  
610 results are helpful to understand the browning inhibition mechanism conferred by H<sub>2</sub>S  
611 on fresh-cut apple, which is beneficial for the technological innovation of browning  
612 prevention and amelioration for fresh-cut fruit.

613

614 **Funding:** The work was financially supported by National Key R&D Program of  
615 China (2016YFD0400903) and the National Natural Science Foundation of China  
616 (31601517, 31801598).

617

618 **Notes:**

619 The authors declare no competing financial interest.

620

621 **References:**

622

623 Amaki, K., Saito, E., Taniguchi, K., Joshita, K., Murata, M., 2011. Role of  
624 chlorogenic acid quinone and interaction of chlorogenic acid quinone and catechins in  
625 the enzymatic browning of apple. *Biosci. Biotechnol. Biochem.* 75, 100444-1–4.  
626 DOI:10.1271/bbb.100444

627 AOAC, 1990. Vitamin C (ascorbic acid) in vitamin preparations and juices.  
628 Official methods of analysis, 15th edn. AOAC, Arlington.

629 Boeckx, J., Pols, S., Hertog, M.L., Nicolai, B.M., 2019. Regulation of the central  
630 carbon metabolism in apple fruit exposed to postharvest low-oxygen stress. *Front.*  
631 *Plant Sci.* 10, 1384. DOI:10.3389/fpls.2019.01384

632 Cantos, E., Tudela, J.A., Gil, M.I., Espín, J.C., 2002. Phenolic compounds and  
633 related enzymes are not rate-limiting in browning development of fresh-cut potatoes. *J.*  
634 *Agric. Food Chem.* 50, 3015–3023. DOI:10.1021/jf0116350

635 Chen, C., Hu, W., He, Y., Jiang, A., Zhang, R., 2016a. Effect of citric acid  
636 combined with UV-C on the quality of fresh-cut apple. *Postharvest Biol. Technol.* 111,  
637 126–131. DOI:10.1016/j.postharvbio.2015.08.005

638 Chen, C., Hu, W., Zhang, R., Jiang, A., Zou, Y., 2016b. Levels of phenolic  
639 compounds, antioxidant capacity, and microbial counts of fresh-cut onions after  
640 treatment with a combination of nisin and citric acid. *Hortic. Environ. Biotechnol.* 57,  
641 266–273. DOI:10.1007/s13580-016-0032-x

642 Chi, M., Bhagwat, B., Lane, W.D., Tang, G., Su, Y., Sun, R., Oomah, B.D.,  
643 Wiersma, P.A., Xiang, Y., 2014. Reduced polyphenol oxidase gene expression and

644 enzymatic browning in potato (*Solanum tuberosum* L.) with artificial microRNAs.  
645 BMC Plant Biol. 14, 62. DOI:10.1186/1471-2229-14-62

646 Cocetta, G., Baldassarre, V., Spinardi, A., Ferrante, A., 2014. Effect of cutting on  
647 ascorbic acid oxidation and recycling in fresh-cut baby spinach (*Spinacia oleracea* L.)  
648 leaves. Postharvest Biol. Technol. 88, 8–16. DOI:10.1016/j.postharvbio.2013.09.001

649 Coetzer, C., Corsini, D., Love, S., Pavek, J., Tumer, N., 2001. Control of  
650 enzymatic browning in potato (*Solanum tuberosum* L.) by sense and antisense RNA  
651 from tomato polyphenol oxidase. J. Agric. Food Chem. 49, 652–657.  
652 DOI:10.1021/jf001217f

653 Degl'Innocenti, E., Guidi, L., Pardossi, A., Tognoni, F., 2005. Biochemical study  
654 of leaf browning in minimally processed leaves of lettuce (*Lactuca sativa* L. var.  
655 Acephala). J. Agric. Food Chem. 53, 9980–9984. DOI:10.1021/jf050927o

656 Docimo, T., Francese, G., De Palma, M., Mennella, D., Toppino, L., Lo Scalzo,  
657 R., Mennella, G., Tucci, M., 2016. Insights in the fruit flesh browning mechanisms in  
658 *Solanum melongena* genetic lines with opposite postcut behavior. J. Agric. Food  
659 Chem. 64, 4675–4685. DOI:10.1021/acs.jafc.6b00662

660 Dong, T., Cao, Y., Jiang, C.-Z., Li, G., Liu, P., Liu, S., Wang, Q., 2020. Cysteine  
661 protease inhibitors reduce enzymatic browning of potato by lowering the  
662 accumulation of free amino acids. J. Agric. Food Chem. 68, 2467–2476.  
663 DOI:10.1021/acs.jafc.9b07541

664 Franck, C., Lammertyn, J., Ho, Q.T., Verboven, P., Verlinden, B., Nicolai, B.M.,  
665 2007. Browning disorders in pear fruit. Postharvest Biol. Technol. 43, 1–13.  
666 DOI:10.1016/j.postharvbio.2006.08.008

667 Frazee, A.C., Perteza, G., Jaffe, A.E., Langmead, B., Salzberg, S.L., Leek, J.T.,  
668 2015. Ballgown bridges the gap between transcriptome assembly and expression  
669 analysis. *Nat. Biotechnol.* 33, 243–246. DOI:10.1038/nbt.3172

670 Gao, S.-P., Hu, K.-D., Hu, L.-Y., Li, Y.-H., Han, Y., Wang, H.-L., Lv, K., Liu,  
671 Y.-S., Zhang, H., 2013. Hydrogen sulfide delays postharvest senescence and plays an  
672 antioxidative role in fresh-cut kiwifruit. *HortScience* 48, 1385–1392.  
673 DOI:10.21273/HORTSCI.48.11.1385

674 Giovinazzo et al., 2021. Hydrogen sulfide is neuroprotective in Alzheimer's  
675 disease by sulfhydrating GSK3 $\beta$  and inhibiting Tau hyperphosphorylation. *PNAS*  
676 118(4), e2017225118. DOI:10.1073/pnas.2017225118

677 Guan, W., Fan, X., 2010. Combination of sodium chlorite and calcium  
678 propionate reduces enzymatic browning and microbial population of fresh-cut  
679 "Granny Smith" apple. *J. Food Sci.* 75, M72–M77.  
680 DOI:10.1111/j.1750-3841.2009.01470.x

681 Hancock, J.T., Whiteman, M., 2014. Hydrogen sulfide and cell signaling: team  
682 player or referee? *Plant Physiol. Biochem.* 78, 37–42.  
683 DOI:10.1016/j.plaphy.2014.02.012

684 Hemachandran, H., Anantharaman, A., Mohan, S., Mohan, G., Kumar, D.T., Dey,  
685 D., Kumar, D., Dey, P., Choudhury, A., Doss, C.G.P., 2017. Unraveling the inhibition  
686 mechanism of cyanidin-3-sophoroside on polyphenol oxidase and its effect on  
687 enzymatic browning of apple. *Food Chem.* 227, 102–110.  
688 DOI:10.1016/j.foodchem.2017.01.041

689 Hu, Hu, S.-L., Wu, J., Li, Y.-H., Zheng, J.-L., Wei, Z.-J., Liu, J., Wang, H.-L.,  
690 Liu, Y.-S., Zhang, H., 2012. Hydrogen sulfide prolongs postharvest shelf life of

691 strawberry and plays an antioxidative role in fruits. *J. Agric. Food Chem.* 60,  
692 8684–8693. DOI:10.1021/jf300728h

693 Hu, Wang, Q., Hu, L.-Y., Gao, S.-P., Wu, J., Li, Y.-H., Zheng, J.-L., Han, Y., Liu,  
694 Y.-S., Zhang, H., 2014b. Hydrogen sulfide prolongs postharvest storage of fresh-cut  
695 pears (*Pyrus pyrifolia*) by alleviation of oxidative damage and inhibition of fungal  
696 growth. *PloS one* 9, e85524. DOI:10.1371/journal.pone.0085524

697 Hu, H., Shen, W., Li, P., 2014a. Effects of hydrogen sulphide on quality and  
698 antioxidant capacity of mulberry fruit. *Int. J. Food Sci. Tech.* 49, 399–409.  
699 DOI:10.1111/ijfs.12313

700 Jiang, J., Jiang, L., Zhang, L., Luo, H., Opiyo, A.M., Yu, Z., 2012. Changes of  
701 protein profile in fresh-cut lotus tuber before and after browning. *J. Agric. Food Chem.*  
702 60, 3955–3965. DOI:10.1021/jf205303y

703 Jin, Z., Pei, Y., 2015. Physiological implications of hydrogen sulfide in plants:  
704 pleasant exploration behind its unpleasant odour. *Oxid Med Cell Longev.* 397502.  
705 DOI:10.1155/2015/397502

706 Kim, D., Langmead, B., Salzberg, S.L., 2015. HISAT: a fast spliced aligner with  
707 low memory requirements. *Nat. Methods* 12, 357–360. DOI:10.1038/nmeth.3317

708 Landrigan, M., Morris, S., Eamus, D., McGlasson, W., 1996. Postharvest water  
709 relationships and tissue browning of rambutan fruit. *Sci. Horticult.* 66, 201-208.  
710 DOI:10.1016/S0304-4238(96)00915-6

711 Li, Z., Zhang, Y., Ge, H., 2017. The membrane may be an important factor in  
712 browning of fresh-cut pear. *Food Chem.* 230, 265–270. DOI:  
713 10.1016/j.foodchem.2017.03.044

714 Liang, D., Wang, C., Tocmo, R., Wu, H., Deng, L.-W., Huang, D., 2015.  
715 Hydrogen sulphide (H<sub>2</sub>S) releasing capacity of essential oils isolated from

716 organosulphur rich fruits and vegetables. *J. Funct. Foods* 14, 634–640.  
717 DOI:10.1016/j.jff.2015.02.007

718 Lin, Y., Lin, Y., Lin, H., Chen, Y., Wang, H., Shi, J., 2018. Application of propyl  
719 gallate alleviates pericarp browning in harvested longan fruit by modulating  
720 metabolisms of respiration and energy. *Food Chem.* 240, 863–869.  
721 DOI:10.1016/j.foodchem.2017.07.118

722 Liu, X., Yang, Q., Lu, Y., Li, Y., Li, T., Zhou, B., Qiao, L., 2019. Effect of  
723 purslane (*Portulaca oleracea* L.) extract on anti-browning of fresh-cut potato slices  
724 during storage. *Food Chem.* 283, 445–453. DOI:10.1016/j.foodchem.2019.01.058

725 Livak, K.J., Schmittgen, T.D., 2001. Analysis of relative gene expression data  
726 using real-time quantitative PCR and the 2<sup>-</sup> ΔΔCT method. *Methods* 25, 402–408.  
727 DOI:10.1006/meth.2001.1262

728 Mellidou, I., Buts, K., Hatoum, D., Ho, Q.T., Johnston, J.W., Watkins, C.B.,  
729 Schaffer, R.J., Gapper, N.E., Giovannoni, J.J., Rudell, D.R., 2014. Transcriptomic  
730 events associated with internal browning of apple during postharvest storage. *BMC*  
731 *Plant Biol.* 14, 328. DOI:10.1186/s12870-014-0328-x

732 Mellidou, I., Kanellis, A.K., 2017. Genetic control of ascorbic acid biosynthesis  
733 and recycling in horticultural crops. *Front. Chem.* 5, 50.  
734 DOI:10.3389/fchem.2017.00050

735 Milani, J., Hamed, M., 2004. Susceptibility of five apple cultivars to enzymatic  
736 browning, V *International Postharvest Symposium* 682, 2221–2226.  
737 DOI:10.17660/ActaHortic.2005.682.303

738 Møller, I.M., 2001. Plant mitochondria and oxidative stress: electron transport,  
739 NADPH turnover, and metabolism of reactive oxygen species. *Annu. Rev. Plant Biol.*  
740 52, 561–591. DOI:10.1146/annurev.arplant.52.1.561



741 Palou, E., López-Malo, A., Barbosa-Cánovas, G., Welti-Chanes, J., Swanson, B.,  
742 1999. Polyphenoloxidase activity and color of blanched and high hydrostatic pressure  
743 treated banana puree. *J. Food Sci.* 64, 42–45.  
744 DOI:10.1111/j.1365-2621.1999.tb09857.x

745 Patterson, B.D., MacRae, E.A., Ferguson, I.B., 1984. Estimation of hydrogen  
746 peroxide in plant extracts using titanium (IV). *Anal. Biochem.* 139, 487–492.  
747 DOI:10.1016/0003-2697(84)90039-3

748 Perteua, M., Perteua, G.M., Antonescu, C.M., Chang, T.-C., Mendell, J.T., Salzberg,  
749 S.L., 2015. StringTie enables improved reconstruction of a transcriptome from  
750 RNA-seq reads. *Nat. Biotechnol.* 33, 290–295. DOI:10.1038/nbt.3122

751 Rawyler, A., Pavelic, D., Gianinazzi, C., Oberson, J., Braendle, R., 1999.  
752 Membrane lipid integrity relies on a threshold of ATP production rate in potato cell  
753 cultures submitted to anoxia. *Plant Physiol.* 120, 293–300. DOI:10.1104/pp.120.1.293

754 Ren, Y., Wang, Y., Bi, Y., Ge, Y., Wang, Y., Fan, C., Li, D., Deng, H., 2012.  
755 Postharvest BTH treatment induced disease resistance and enhanced reactive oxygen  
756 species metabolism in muskmelon (*Cucumis melo* L.) fruit. *Eur. Food Res. Technol.*  
757 234, 963–971. DOI:10.1007/s00217-012-1715-x

758 Reyes, L.F., Villarreal, J.E., Cisneros-Zevallos, L., 2007. The increase in  
759 antioxidant capacity after wounding depends on the type of fruit or vegetable tissue.  
760 *Food Chem.* 101, 1254–1262. DOI:10.1016/j.foodchem.2006.03.032

761 Richard-Forget, F.C., Gaillard, F.A., 1997. Oxidation of chlorogenic acid,  
762 catechins, and 4-methylcatechol in model solutions by combinations of pear (*Pyrus*  
763 *communis* cv. Williams) polyphenol oxidase and peroxidase: a possible involvement  
764 of peroxidase in enzymatic browning. *J. Agric. Food Chem.* 45, 2472–2476.  
765 10.1021/jf970042f

766 Saba, M.K., Sogvar, O.B., 2016. Combination of carboxymethyl cellulose-based  
767 coatings with calcium and ascorbic acid impacts in browning and quality of fresh-cut  
768 apple. *LWT-Food Science and Technology* 66, 165–171. DOI:  
769 10.1016/j.lwt.2015.10.022

770 Saltveit, M.E., 2000. Wound induced changes in phenolic metabolism and tissue  
771 browning are altered by heat shock. *Postharvest Biol. Technol.* 21, 61–69.  
772 DOI:10.1016/S0925-5214(00)00165-4

773 Saquet, A.A., Streif, J., Bangerth, F., 2003. Energy metabolism and membrane  
774 lipid alterations in relation to brown heart development in ‘Conference’ pears during  
775 delayed controlled atmosphere storage. *Postharvest Biol. Technol.* 30, 123–132.  
776 DOI:10.1016/S0925-5214(03)00099-1

777 Shrestha, L., Kulig, B., Moschetti, R., Massantini, R., Pawelzik, E., Hensel, O.,  
778 Sturm, B., 2020. Optimisation of Physical and Chemical Treatments to Control  
779 Browning Development and Enzymatic Activity on Fresh-cut Apple Slices. *Foods* 9,  
780 76. DOI:10.3390/foods9010076

781 Sun, Y., Zhang, W., Zeng, T., Nie, Q., Zhang, F., Zhu, L., 2015. Hydrogen sulfide  
782 inhibits enzymatic browning of fresh-cut lotus root slices by regulating phenolic  
783 metabolism. *Food Chem.* 177, 376–381. DOI:10.1016/j.foodchem.2015.01.065

784 Toivonen, P.M.A., Brummell, D.A., 2008. Biochemical bases of appearance and  
785 texture changes in fresh-cut fruit and vegetables. *Postharvest Biol. Technol.* 48, 1–14.  
786 DOI:10.1016/j.postharvbio.2007.09.004

787 Wang, 2002. Two’s company, three’s a crowd: can H<sub>2</sub>S be the third endogenous  
788 gaseous transmitter? *FASEB Journal* 16, 1792–1798. DOI:org/10.1096/fj.02-0211hyp

789 Wang, J., Lv, M., Li, G., Jiang, Y., Fu, W., Zhang, L., Ji, S., 2018. Effect of  
790 intermittent warming on alleviation of peel browning of ‘Nanguo’ pears by regulation

791 energy and lipid metabolisms after cold storage. *Postharvest Biol. Technol.* 142,  
792 99–106. DOI:10.1016/j.postharvbio.2017.12.007

793 Xu, C., Zeng, B., Huang, J., Huang, W., Liu, Y., 2015. Genome-wide  
794 transcriptome and expression profile analysis of *Phalaenopsis* during explant  
795 browning. *PloS one* 10, e0123356. DOI:10.1371/journal.pone.0123356

796 Yan, S., Luo, Y., Zhou, B., Ingram, D.T., 2017. Dual effectiveness of ascorbic  
797 acid and ethanol combined treatment to inhibit browning and inactivate pathogens on  
798 fresh-cut apple. *LWT-Food Sci. Technol.* 80, 311–320.  
799 DOI:10.1016/j.lwt.2017.02.021

800 Yin, Y., Bi, Y., Li, Y., Wang, Y., Wang, D., 2012. Use of thiamine for controlling  
801 *Alternaria alternata* postharvest rot in Asian pear (*Pyrus bretschneideri* Rehd. cv.  
802 Zaosu). *Int. J. Food Sci. Tech.* 47, 2190–2197.  
803 DOI:10.1111/j.1365-2621.2012.03088.x

804 Zhang, J., Yuan, L., Liu, W., Lin, Q., Wang, Z., Guan, W., 2017. Effects of UV-C  
805 on antioxidant capacity, antioxidant enzyme activity and colour of fresh-cut red  
806 cabbage during storage. *Int. J. Food Sci. Tech.* 52, 626–634. DOI:10.1111/ijfs.13315

807 Zhang, S., Lin, Y., Lin, H., Lin, Y., Chen, Y., Wang, H., Shi, J., Lin, Y., 2018.  
808 *Lasiodiplodia theobromae* (Pat.) Griff. & Maubl. -induced disease development and  
809 pericarp browning of harvested longan fruit in association with membrane lipids  
810 metabolism. *Food Chem.* 244, 93–101. DOI:10.1016/j.foodchem.2017.10.020

811 Zhang, S., Tian, L., Zhang, Y., Zhao, H., Zhao, J., Guo, J., Zhu, G.-P., 2019. *De*  
812 *novo* transcriptome assembly of the fresh-cut white husk of *Juglans cathayensis* Dode:  
813 insights for enzymatic browning mechanism of fresh-cut husk of walnut. *Sci. Horticult.*  
814 257, 108654. 10.1016/j.scienta.2019.108654

815 Zheng, J.-L., Hu, L.-Y., Hu, K.-D., Wu, J., Yang, F., Zhang, H., 2016. Hydrogen  
816 sulfide alleviates senescence of fresh-cut apple by regulating antioxidant defense  
817 system and senescence-related gene expression. HortScience 51, 152–158.  
818 DOI:10.21273/HORTSCI.51.2.152

819 Zhu, H., Liu, J., Wen, Q., Chen, M., Wang, B., Zhang, Q., Xue, Z., 2017. De  
820 novo sequencing and analysis of the transcriptome during the browning of fresh-cut  
821 *Luffa cylindrica* 'Fusi-3' fruits. PloS one 12. DOI:10.1371/journal.pone.0187117

822 **Figures**

823 Fig. 1 Effects of H<sub>2</sub>S treatment on the (A) appearance and (B) browning index of  
824 fresh-cut apple during storage at 4 °C.

825 Fig. 2 Physiological changes of fresh-cut apple after H<sub>2</sub>S treatment during storage at  
826 4 °C. (A) PPO, (B) POD, (C) PAL, (D) SOD, (E) CAT, (F) APX and (G) GR activities,  
827 (H) H<sub>2</sub>O<sub>2</sub> content, (I) AsA content, (J) phenolic content.

828 Fig. 3 Differentially Expressed Genes (DEGs) between samples. (A) Numbers of up-  
829 and down-regulated DEGs in S0 vs. C0, S6 vs. C6, C6 vs. C0 and S6 vs. S0. Venn  
830 diagrams showing common DEGs in S0 vs. C0 and S6 vs. C6 (B), C6 vs. C0 and S6  
831 vs. S0 (C).

832 Fig. 4 The top 15 enriched GO terms ( $P < 0.05$ ) of biological process, cellular  
833 component and molecular function in S0 vs. C0 (A), S6 vs. C6 (B), C6 vs. C0 (C) and  
834 S6 vs. S0 (D).

835 Fig. 5 Proposed model for the browning inhibition of fresh-cut apple by H<sub>2</sub>S.

836 Fig. 6 Correlation analysis between RNA-seq and qRT-PCR data.

837 **Supplementary material**

838 Fig. S1 Gene expression pattern of the DEGs of the control and H<sub>2</sub>S treatment at day

839 6 relative to day 0 in the common GO terms.

840 Table S1 Primers used in qRT-PCR for the validation of RNA-Seq data.

841 Table S2 Quality summary of sequencing data.

842 Table S3 The number of unigene and transcript identified in each sample.

843 Table S4 Uniquely expressed genes in each samples.

844 Table S5 Top 10 up- and down-regulated genes after H<sub>2</sub>S treatment.

845 Table S6 KEGG pathway classification of the DEGs in S0 vs. C0, S6 vs. C6, C6 vs.

846 C0 and S6 vs. S0

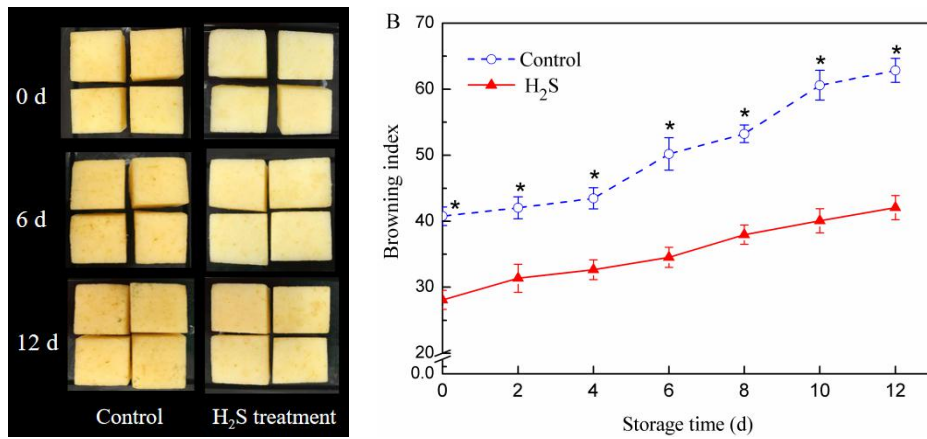
847 Table S7 DEGs involved in fatty acid metabolism.

848 Table S8 DEGs involved in Glycerophospholipid metabolism.

849 Table S9 DEGs involved in oxidative phosphorylation.

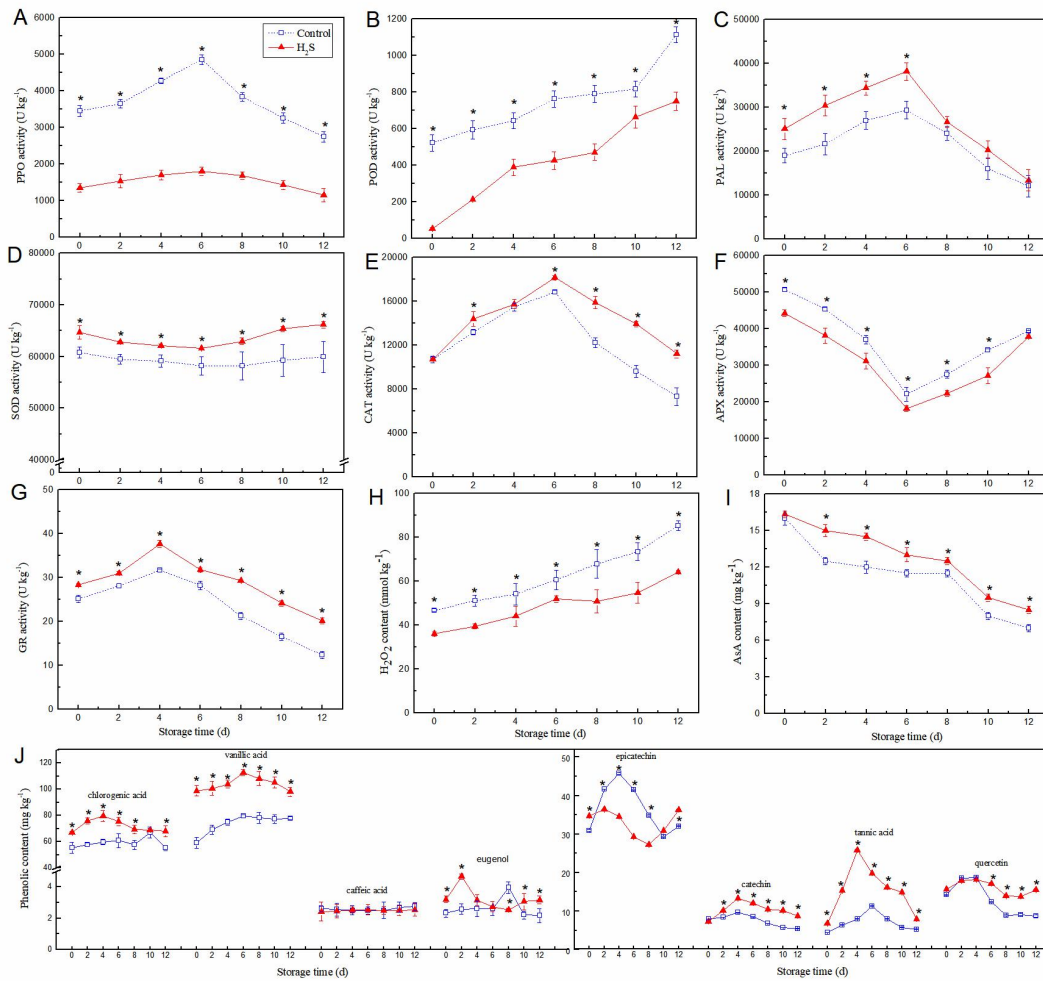
850 Table S10 DEGs involved in glycolysis.

851 Table S11 DEGs involved in TCA.



1

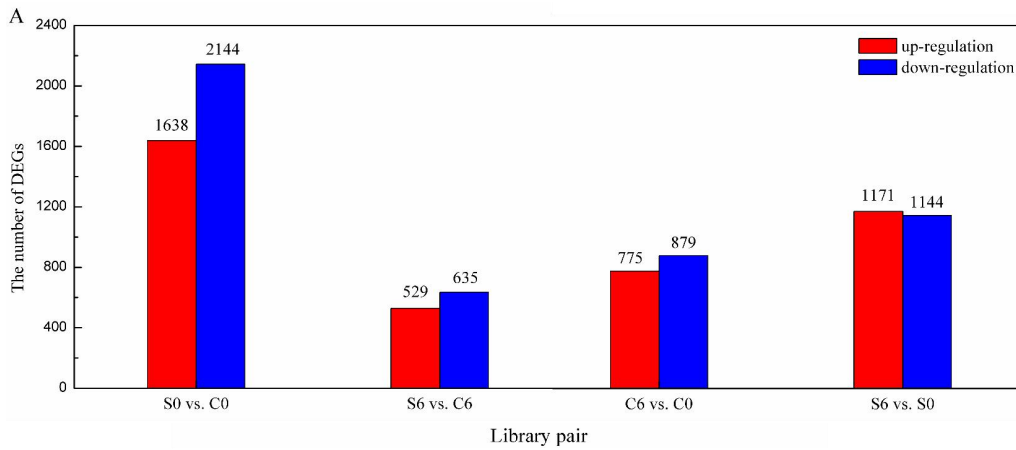
2 Fig. 1 Effects of H<sub>2</sub>S treatment on the (A) appearance and (B) browning index of  
 3 fresh-cut apple during storage at 4 °C. The error bars represent standard deviation (SD,  
 4 n = 3). \*: statistically significant differences (P < 0.05).



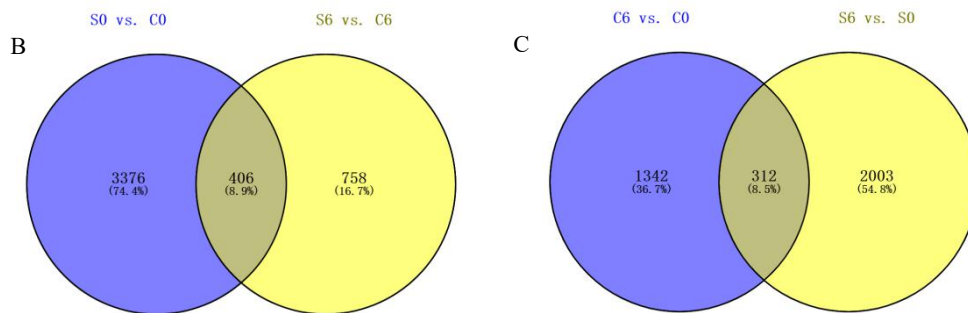
5

6 Fig. 2 Physiological changes of fresh-cut apple after H<sub>2</sub>S treatment during storage at  
 7 4 °C. (A) PPO, (B) POD, (C) PAL, (D) SOD, (E) CAT, (F) APX and (G) GR activities,  
 8 (H) H<sub>2</sub>O<sub>2</sub> content, (I) AsA content, (J) phenolic content. The error bars represent  
 9 standard deviation (SD, n = 3). \*: statistically significant differences (P < 0.05).



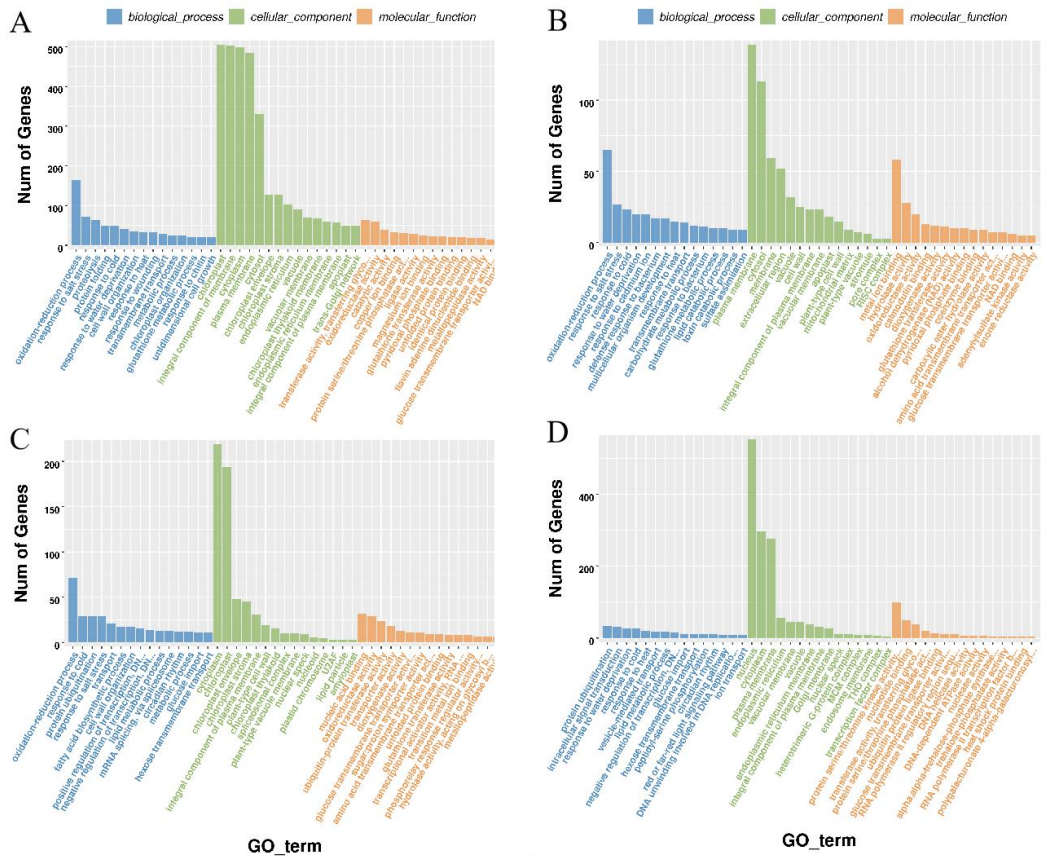


10



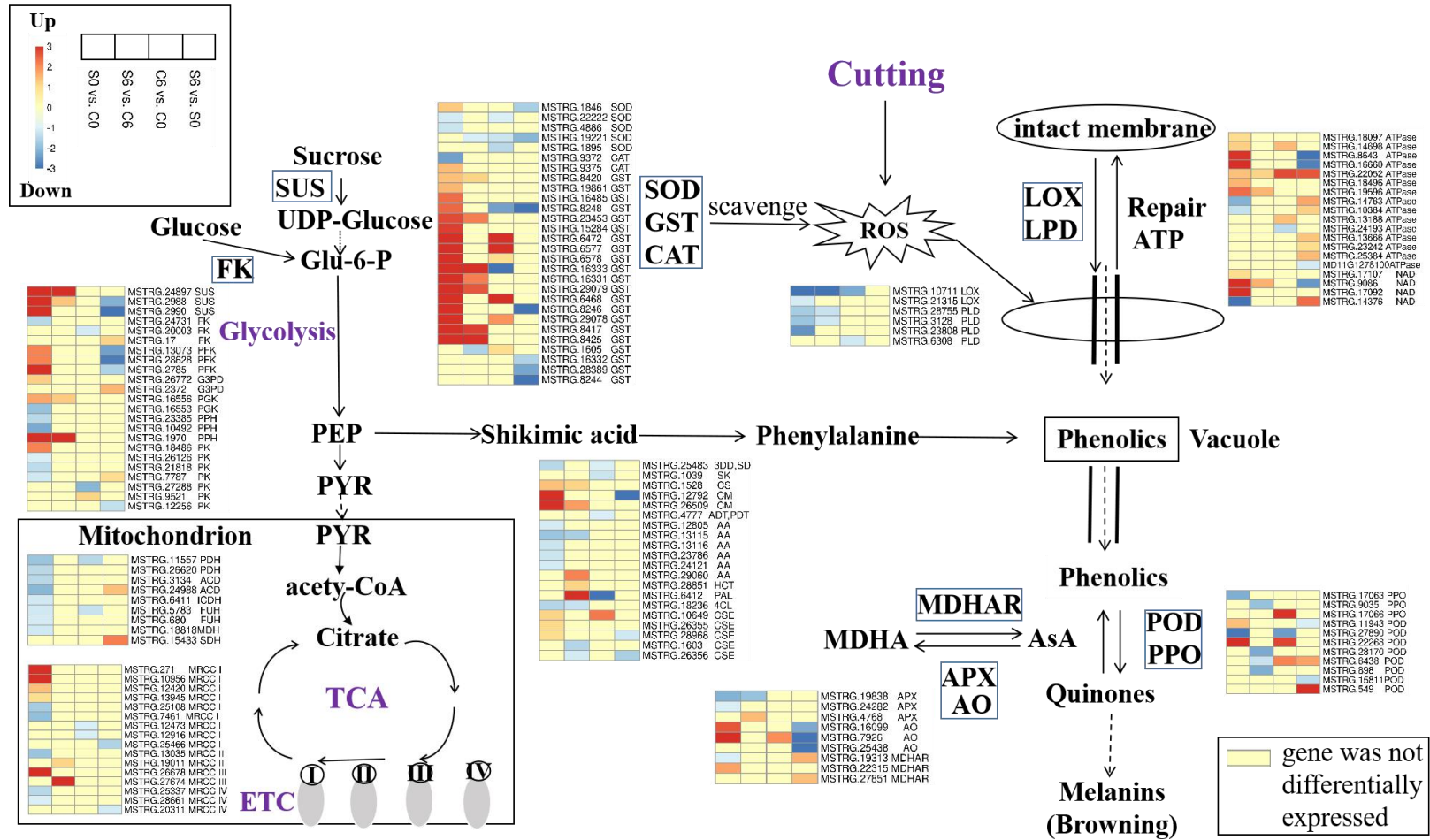
11

12 Fig. 3 Differentially Expressed Genes (DEGs) between samples. (A) Numbers of up-  
 13 and down-regulated DEGs in S0 vs. C0, S6 vs. C6, C6 vs. C0 and S6 vs. S0. Venn  
 14 diagrams showing common DEGs in (B) S0 vs. C0 and S6 vs. C6, (C) C6 vs. C0 and  
 15 S6 vs. S0. DEGs were filtered with a cut-off of  $|\log_2FC| \geq 1$  and  $P < 0.05$ .



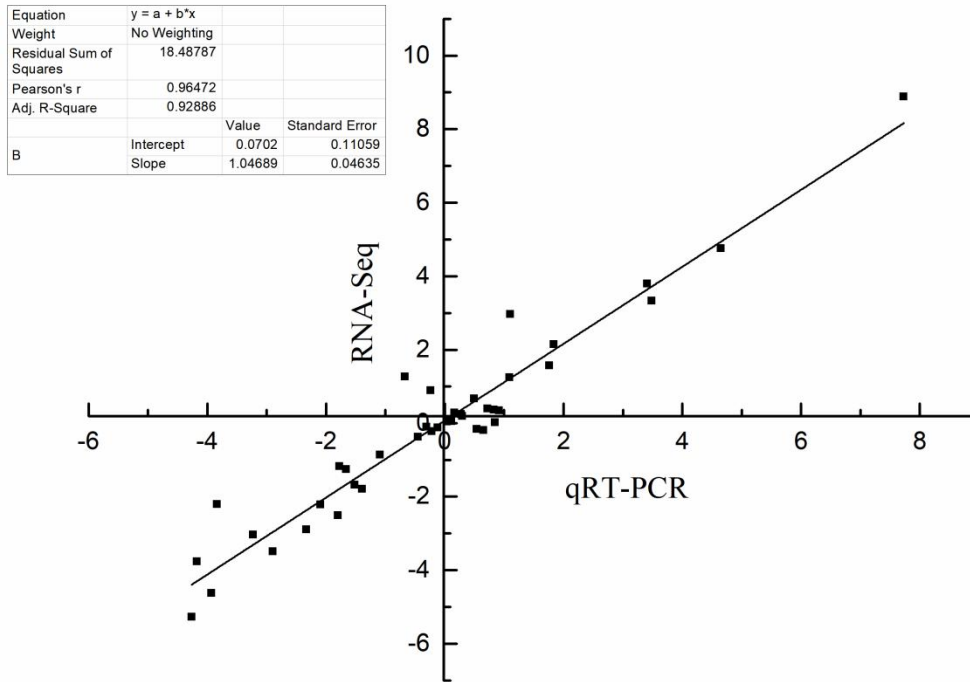
16

17 Fig. 4 The top 15 enriched GO terms ( $P < 0.05$ ) of biological process, cellular  
 18 component and molecular function in (A) S0 vs. C0, (B) S6 vs. C6, (C) C6 vs. C0 and  
 19 (D) S6 vs. S0.



22 Fig. 5 Proposed model for the browning inhibition of fresh-cut apple by H<sub>2</sub>S. Heat maps representing the expression patterns of DEGs, yellow

23 means gene was not differentially expressed ( $P \geq 0.05$  or  $-1 < \log_2FC < 1$ ). 3DD,SD: bifunctional 3-dehydroquininate dehydratase/shikimate  
24 dehydrogenase, 4CL: 4-coumarate-CoA ligase, AA: aspartate aminotransferase, ACD: aconitate hydratase, ADT,PDT: arogenate  
25 dehydratase/prephenate dehydratase, AO: ascorbate oxidase, APX: ascorbate peroxidase, AsA: ascorbic acid, CAT: catalase, CM: chorismate  
26 mutase, CS: chorismate synthase, FK: fructokinase, FUH: fumarate hydratase, G3PD: glyceraldehyde-3-phosphate dehydrogenase, GST:  
27 glutathione S-transferase, HCT: shikimate O-hydroxycinnamoyltransferase, ICDH: isocitrate dehydrogenase, LOX: lipoxidase, LPD:  
28 phospholipase D, MDH: malate dehydrogenase, MDHAR: monodehydroascorbate reductase, NAD: NADH dehydrogenase, PAL: phenylalanine  
29 ammonia-lyase, PDH: pyruvate dehydrogenase, PFK: 6-phosphofructokinase, PGK: phosphoglycerate kinase, PK: pyruvate kinase, POD:  
30 peroxidase, PPH: phosphopyruvate hydratase, PPO: polyphenol oxidase, SOD: superoxide dismutase, SDH: succinate dehydrogenase, SUS:  
31 sucrose synthase, SK: shikimate kinase.



32

33 Fig. 6 Correlation analysis between RNA-seq and qRT-PCR data. Ten DEGs from the  
 34 RNA-seq assay were used for qRT-PCR assay. The  $\log_2FC$  obtained by qRT-PCR  
 35 (X-axis) was plotted against  $\log_2FC$  by RNA-seq (Y-axis).